Electronic properties of a quasi-two-dimensional electron gas in semiconductor quantum wells under intense laser fields

B. G. Enders,[1] F. M. S. Lima,[1] O. A. C. Nunes,[1,*] A. L. A. Fonseca,[1] D. A. Agrello,[1] Fanyao Qu,[2] E. F. Da Silva, Jr.,[3] and V. N. Freire[4]

[1]*Instituto de Física, Universidade de Brasília, P.O. Box 04455, 70919-970, Brasília, Distrito Federal, DF, Brazil*

[2]*Departamento de Ciências Físicas, Universidade Federal de Uberlândia, 38400-902, Uberlândia, MG, Brazil*

[3]*Departamento de Física, Universidade Federal de Pernambuco, Cidade Universitária, Recife, PE, 50670-901, Brazil*

[4]*Departamento de Física, Universidade Federal do Ceará, Campus do Pici, 60455-970, Fortaleza, CE, Brazil*

(Received 24 October 2003; revised manuscript received 11 March 2004; published 15 July 2004)

A systematic study on the influence of two intense, long-wavelength, nonresonant laser fields on the electron energy levels and density of states (DOS) in GaAs/AlGaAs quantum wells is performed within a Green's function approach. The carrier confinement pattern and its associated DOS are shown to be modified by the laser beams. For laser field polarizations parallel to the growth direction only the effective potential is changed whereas for in-plane polarizations only the DOS is altered in the sense that it is field-driven. The results show that for a GaAs/AlGaAs quantum well the effect of the laser field radiation is to induce strong blueshifts in the electronic energy levels. The DOS dependence on the laser-induced confinement characteristics changes from the usual ladder profile to a functional form that reminds us of a one-dimensional system.

DOI: 10.1103/PhysRevB.70.035307 PACS number(s): 73.63.−b, 73.20.At, 78.30.Fs, 78.67.De

I. INTRODUCTION

With the advent of high-power, long-wavelength, linearly polarized laser sources possibilities have arisen in the study of the interaction of intense laser fields (ILFs) with electrons in semiconductors.[1–3] In the case of semiconductor heterostructures, the situation is even more interesting due to the possibility of carrier confinement within more than one nanometrical distance, thus reducing the dimensionality of the system. Recently, this possibility has been investigated with the use of high-quality, tunable laser sources, such as CO_2 and free-electron lasers (FEL), applied to low-dimensional electronic system samples.[4] As a consequence, some important and distinctive phenomena associated with laser-driven two-dimensional electron gases (2DEGs) have been theoretically anticipated[5,6] and observed.[4,7]

Theoretical calculations of the changes induced by an ILF on the first subband energy level[8] and mobility[9] for electrons in a quantum well (QW), and on the binding energy of a hydrogenic impurity confined in a QW (Ref. 10) were already developed. The terahertz (THz) assisted electron-phonon and electron-impurity scattering rates for electrons in a single heterojunction have been calculated by Cao and Lei in a recent paper.[11] Essentially the same formalism was considered in the study of tuning mechanisms for laser emission[8] and laser-driven resonant tunneling[12] in a double-barrier heterostructure. In the case of modulation-doped quantum wells, a similar tunability was found for the 2DEG areal density.[13] In fact, in the presence of a linearly polarized electromagnetic (EM) radiation, modifications in the electron density of states (DOS) in three-dimensional electron gases[6,14] (3DEG) and *ideal* 2DEG (Ref. 6) systems were systematically investigated, leading to the theoretical prediction of the dynamic Franz-Keldysh effect (DFKE),[6] which was detected recently.[15]

In the case of a *quasi*-2DEG, i.e., an electron gas confined in a well slab with finite width, important effects of THz laser radiation were found for the DOS dependence on the electron energy in QWs modeled with both infinite[16] and finite[17] barrier heights. In these works, the author treated the electron-photon interaction exactly, using the standard gauge-invariant spectral function and considering the most general case of laser beams composed of resonant photons, thus taking into account both absorption and emission processes. As a consequence, the summations and integrals involved in the expressions obtained for the correction of the DOS due to the presence of laser fields are too voluminous.[18] Nevertheless, the possibility of obtaining modifications on the electronic structure of a laser-driven quasi-2DEG confined in a QW with finite width and barrier heights by using only nonresonant[19] laser beams was not explored, despite the fact that the mathematical expressions involved are much simpler. Since the DOS is one of the central quantities for calculating almost all physically measurable properties, in this paper we have considered as relevant the task of investigating in detail the changes induced in this quantity by illuminating a QW with an intense, nonresonant laser source. Moreover, the possibility of enhancing the laser-induced blueshift on the electron energy levels by simultaneously applying two linearly polarized laser beams in a crossed configuration was not investigated to date. We have also judged it important to examine how the presence of intense, long-wavelength, nonresonant laser fields affects the potential profile, the energy levels, and the DOS, simultaneously, for electrons confined in a single QW.

The paper is organized as follows. In Sec. II we present the mathematical formalism concerning the calculation of the electronic structure for noninteracting quasi-2D electrons confined in a semiconductor QW in the presence of intense, long-wavelength, nonresonant laser fields. Emphasis will be given on the bound state energy levels and on the DOS dependence on the energy. In Sec. III the numerical results for

a GaAs/AlGaAs single QW are presented and discussed. The possibility of tuning both the DOS and the energy levels in quasi-2D electronic systems by varying the laser frequency and/or intensity is pointed out for a CO_2 beam propagating perpendicularly to a THz beam, which is propagating along the growth direction. Concluding remarks are given in Sec. IV.

II. ELECTRONIC STRUCTURE CALCULATION

In the absence of EM radiations, the energy levels and the DOS can be easily computed for quasi-2D electrons confined in QWs with barriers of finite height and within the effective mass approximation. In this case, the well potential reads

$$V_0(z) = V_0(|z| - L/2), \tag{1}$$

where V_0 is the barrier height, $\Theta(z)$ is the Heaviside step function, and L is the well width. If we let the z axis be perpendicular to the QW interfaces the quasi-2D electron wave function is given by[20–22]

$$\psi_{n,\mathbf{k}}(\mathbf{r}_\perp, z) = \frac{1}{\sqrt{S}} e^{i\mathbf{k}\cdot\mathbf{r}_\perp} \chi_n(z), \tag{2}$$

where S is the normalization area, $\mathbf{r}_\perp \equiv x\hat{x} + y\hat{y}$ is the in-plane position, and $\mathbf{k} \equiv k_x\hat{x} + k_y\hat{y}$ is the in-plane wave vector. Each subband is identified by the index $n(=1,2,\ldots)$ so $\chi_n(z)$ and ε_n are the envelope wave function and their corresponding bound state energy levels, respectively; the energy spectrum being given by $E_n(\mathbf{k}) = \varepsilon_n + \hbar^2\mathbf{k}^2/(2m^*)$. In the case of undoped QWs, the energies ε_n are the eigenvalues of a simple Hamiltonian operator describing the electron motion in a square quantum well. These eigenvalues are the solutions of some transcendental equations that arise from the matching conditions for $\chi_n(z)$ and $[1/m^*(z)](\partial\chi_n/\partial z)$ at the heterointerfaces.[20,22] The latter boundary condition involves the position-dependent effective mass m_A^* (m_B^*) in the channel (barrier) slab. Once all bound state energy levels are determined, the DOS can be evaluated from its general formulation, namely $\rho(E) = \sum_{\mathbf{k}} \delta[E - \varepsilon(\mathbf{k})]$. For the simple case of 2D electrons in a square QW, this summation generates the following integral expression:[22]

$$\rho(E) = g_s \sum_n \frac{S}{4\pi^2} \int\int \delta\left[E - \varepsilon_n - \frac{\hbar^2}{2m^*}(k_x + k_y)\right] dk_x dk_y, \tag{3}$$

where $g_s(=2)$ is the factor for spin degeneracy and m^* is the average of $m^*(z)$ along the growth direction.[23] The integral in Eq. (3) may be solved in terms of the Heaviside step function by using polar coordinates in the $\mathbf{k}$ space. This reduces the expression for the DOS (per unit of area) to

$$\frac{\rho(E)}{S} \equiv D(E) = \rho_0 \sum_n \Theta(E - \varepsilon_n), \tag{4}$$

where $\rho_0 \equiv g_s m^*/(2\pi\hbar^2)$ is the "natural" unit for this quantity. Equation (4) describes the usual ladder profile for the 2D DOS dependence on the carrier energy in the absence of external fields.[22]

Since we are interested in electrons composing a quasi-2DEG subjected to an intense, long-wavelength, *nonresonant* laser field, the first step of the calculation is to check, for a given QW, if the photon energy is below the band gap of the well material and below the intersubband excitation energy—a condition that ensures the absence of emission and absorption processes. Since, for a given barrier height V_0, the intersubband energy decreases with the increase of the well width,[21] we have established the value of the maximum well width (L_{max}) above which the resonance condition is not observed. Afterwards, we have chosen some $L < L_{max}$ and used it to compute the effective potential and corresponding bound state energy levels, taking into account a nonperturbative approach developed initially to describe the behavior of atoms under ILF conditions.[24] We have considered the space-translated version of the semiclassical, time-dependent Schrödinger (SCD) equation for an electron moving under the combined forces of the square quantum well potential and the laser fields. It was assumed here that the radiation field can be described by the dipole approximation in the physically important region of the space. Under these conditions, the one-electron SCD equation in the momentum gauge reads

$$\left[\frac{1}{2m^*}(\mathbf{p} - e\mathbf{A})^2 + V_0(z)\right]\Psi(\mathbf{r},t) = i\hbar\frac{\partial}{\partial t}\Psi(\mathbf{r},t), \tag{5}$$

where $p = (\hbar/i)\nabla$ is the momentum operator and $\mathbf{A} = \mathbf{A}(t)$ is the vector potential created by the EM radiation. In this work, we are interested only in laser field radiations for which $\mathbf{A}(t)$ is either in-plane, i.e., $\mathbf{A}(t) = A_x(t)\hat{x}$, or parallel to the growth direction, i.e., $\mathbf{A}(t) = A_z(t)\hat{z}$. The temporal dependence was assumed as $A_j(t) = A_{0j}\sin(\omega_j t)$, with $j = x, z$. The vector potential is related to the electric field by $\mathbf{F} = -\partial\mathbf{A}/\partial t$ as usual, and its strength is $A_{0j} = F_{0j}/\omega_j$. In Fig. 1 we indicate the growth direction (z axis) and the polarization direction of each laser beam. The above SCD equation, Eq. (5), is written for a moving frame that follows the field-driven motion of the classical electron (the so-called Kramers reference frame).[24]

The effect of the EM radiation polarized parallel to the z axis on the electronic states can be found by separating the effective potential in two parts: a time-dependent (ac) and a time-independent (dc). The eigenvalues and eigenfunctions of the dc part constitute the quasienergy spectra of the system, whereas the ac part will be treated as a perturbation. The separation of the potential energy follows from a unitary transformation $\Psi(\mathbf{r},t) \xrightarrow{U} \phi(\mathbf{r},t)$, as discussed in detail in some recent works.[12,25] This changes Eq. (5) to

$$\left[-\frac{\hbar^2}{2}\frac{d}{dz}\frac{1}{m^*(z)}\frac{d}{dz} + V[z - \alpha(t)]\right]\phi(z,t) = i\hbar\frac{\partial}{\partial t}\phi(z,t), \tag{6}$$

where $V[z - \alpha(t)] = V_0\Theta[|z - \alpha_{0z}\cos(\omega_z t)| - L/2]$, with $\alpha_{0z} \equiv eA_{0z}/(m^*\omega_z)$, is the time-dependent potential, which has the same form of the bare potential but is translated by an

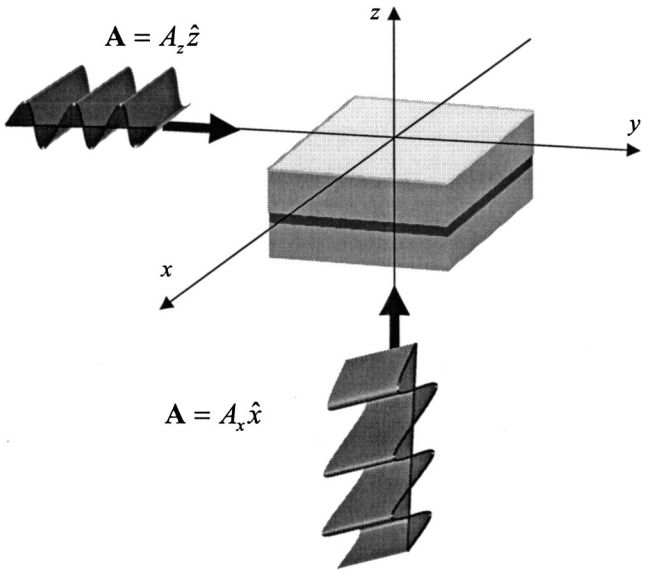

FIG. 1. Heterostructure growth direction (z axis) and polarization/propagation directions for the laser field beams. The dark layer is the GaAs channel, which is sandwiched by two AlGaAs layers (light gray). The dark arrows indicate the propagation directions. Note that the laser radiation propagating along the y axis (z axis) is polarized parallel to the z axis (x axis).

amount $\alpha(t)$ in the z-axis direction (the so-called "laser-dressed" potential).[8,10,26] The displacement $\alpha(t)$, defined as

$$-(e/m^*)\left[\int_0^t A_z(t')dt'\right],$$

is known as the laser-dressing parameter.[10] In the limit $\omega_z\,\tau \gg 1$, the electron motion is dominated by the oscillation of the time-dependent QW potential under the influence of the laser field and, consequently, it "sees" a laser-dressed potential (see Fig. 3 of Ref. 26 for a picture of the physical situation), which is somewhat different from the square potential observed in the absence of external fields. As $V[z-\alpha(t)]$ is a periodic function in time for any position z, these eigenstates can be found by considering the electron as being subjected to a time-averaged potential $\langle V[z-\alpha(t)]\rangle$. Taking this potential into account, the laser-dressed eigenstates are the solutions of

$$\left[-\frac{\hbar^2}{2}\frac{d}{dz}\frac{1}{m^*(z)}\frac{d}{dz}+V_{DC}(z)\right]\phi_m(z)=E_m\phi_m(z). \qquad (7)$$

where $V_{dc}(z)$ is the dominant term (the one of order zero) in the Fourier series expansion of $\langle V[z-\alpha(t)]\rangle$. We solved Eq. (7) numerically, by following an accurate discretization method developed for BenDaniel-Duke type Hamiltonians.[27]

The effect of the in-plane polarized ILF on the electronic states can be obtained by integrating Eq. (5) over t directly, with $\mathbf{A}(t)=A_{0x}\sin(\omega_x t)\hat{x}$. This leads to the following exact time-dependent wave function:

$$\begin{aligned}\Psi_{n,\mathbf{k}}(\mathbf{r},t)=\Psi_{n,\mathbf{k}}(\mathbf{r},0)&\exp\{-i/\hbar[E_n(\mathbf{k})\\&+2\gamma\hbar\omega_x]t\}\exp\{i\alpha_{0x}k_x[1-\cos(\omega_x t)]\}\\&\times\exp[i\gamma\sin(2\omega_x t)],\end{aligned} \qquad (8)$$

where $2\gamma\hbar\omega_x$ is the energy of the laser field, $\mathbf{r}=(\mathbf{r}_\perp,z)$, $\psi_{n,\mathbf{k}}(\mathbf{r},0)=e^{i\mathbf{k}\cdot\mathbf{r}_\perp}\chi_n(z)$, $\alpha_{0x}\equiv eA_{0x}/(m^*\omega_x)$, and $\gamma\equiv e^2A_{0x}^2/(8m^*\hbar\omega_x)$. This electron wave function allows us to separate the time-dependent SCD equation in a time-independent, one-dimensional differential equation describing the motion along the z axis

$$\left\{-\frac{\hbar^2}{2}\frac{d}{dz}\left[\frac{1}{m^*(z)}\frac{d}{dz}\right]+V_0(z)\right\}\chi_n(z)=\varepsilon_n\,\chi_n(z). \qquad (9)$$

The time-dependent wave function in Eq. (8) is related to the probability amplitude of a process in which one adds an electron in a state $|n',\mathbf{k}'\rangle$ at time t' to the system and it evolves to a state $|n,\mathbf{k}\rangle$ at time t. This probability is given by

$$\int d^3r\Psi^*_{n',\mathbf{k}'}(\mathbf{r},t')\Psi_{n,\mathbf{k}}(\mathbf{r},t)=\delta_{n,n'}\delta_{\mathbf{k},\mathbf{k}'}h(n,\mathbf{k};t,t'), \qquad (10)$$

with

$$\begin{aligned}h(n,\mathbf{k};t,t')\equiv&\exp\{-i/\hbar[E_n(\mathbf{k})+2\gamma\hbar\omega_x](t-t')\}\\&\times\exp\{-i\alpha_{0x}k_x[\cos(\omega_x t)-\cos(\omega_x t')]\}\\&\times\exp\{i\gamma[\sin(2\omega_x t)-\sin(2\omega_x t')]\}.\end{aligned} \qquad (11)$$

We now introduce the retarded propagator, or Green's function, in the $(n,\mathbf{k};t)$ space for noninteracting electrons, namely,[28]

$$G^+(n',\mathbf{k}';n,\mathbf{k};t>t')=\delta_{n,n'}\delta_{\mathbf{k},\mathbf{k}'}G^+(n,\mathbf{k};t>t'), \qquad (12)$$

where $G^+(n,\mathbf{k};t>t')=-i/\hbar\Theta(t-t')h(n,\mathbf{k};t,t')$. This is a two-time Green's function, which is the solution of

$$\left[\varepsilon_n+\frac{(\hbar\mathbf{k}-e\mathbf{A})^2}{2m^*}-i\hbar\frac{\partial}{\partial t}\right]G^+(n,\mathbf{k};t>t')=\delta(t'-t) \qquad (13)$$

in the $(n,\mathbf{k};t)$ space and

$$\begin{aligned}\left[\frac{(\mathbf{p}-e\mathbf{A})^2}{2m^*}+V_0(z)-i\hbar\frac{\partial}{\partial t}\right]&G^+(n,\mathbf{k};t>t')\Psi_{n,\mathbf{k}}(\mathbf{r},0)\\&=\delta(t'-t)\Psi_{n,\mathbf{k}}(\mathbf{r},0)\end{aligned} \qquad (14)$$

in the real space, where n and $\mathbf{k}$ are quantum numbers. Then $G^+(n,\mathbf{k};t>t')$ is the actual Green's function in the $(n,\mathbf{k};t)$ space. By converting $e^{ix\cos y}$ and $e^{ix\sin y}$ into Bessel functions, the Fourier transform of the retarded Green's function simplifies to

$$G^{+}_{n,\mathbf{k}}(E,t') = \int_{-\infty}^{+\infty} d(t-t')\exp[i/\hbar(E+i\eta)(t-t')] \times G^{+}(n,\mathbf{k};t>t') = \sum_{m=-\infty}^{+\infty} \frac{\tilde{F}_m(k_x,t')}{E-E_n(\mathbf{k})-2\gamma\hbar\omega_x-m\hbar\omega_x+i\eta}, \tag{15}$$

where the infinitesimal $i\eta$ has been introduced to avoid divergences. The auxiliary function in the summation is given by

$$\tilde{F}_m(k_x,t') = (-1)^m F_m(k_x) \sum_{n=-\infty}^{+\infty} i^n J_{m+n}(\alpha_{0x}k_x) \times \exp\{i[n\omega_x t' - \gamma\sin(2\omega_x t')]\}, \tag{16}$$

where $J_m(x)$ is a Bessel function. The function $F_m(k_x)$ may also be expressed in terms of Bessel functions,

$$F_m(k_x) = \sum_{l=0}^{\infty} \frac{J_l(\gamma)}{1+\delta_{l,0}}[J_{2l-m}(\alpha_{0x}k_x) + (-1)^{m+l}J_{2l+m}(\alpha_{0x}k_x)]. \tag{17}$$

The steady-state properties can be found by averaging the solutions over the initial time t' and averaging t' over a periodicity of the radiation field,[6] i.e., by solving $(\omega_x/2\pi)\int_{-\pi/\omega_x}^{+\pi/\omega_x} dt' G^{+}_{n,\mathbf{k}}(E,t')$. The resulting averaged Green's function is

$$G^{*}_{n,\mathbf{k}}(E) = \sum_{m=-\infty}^{+\infty} \frac{F_m^2(k_x)}{E-E_n(\mathbf{k})-2\gamma\hbar\omega_x-m\hbar\omega_x+i\eta}. \tag{18}$$

It is interesting to note that this complex function is such that $\int dE\ \mathrm{Re}\{G^{*}_{n,\mathbf{k}}(E)\}=0$ and $\int dE\ \mathrm{Im}\{G^{*}_{n,\mathbf{k}}(E)\}=-\pi$, with $\Sigma_{m=-\infty}^{+\infty}F_m^2(k_x)=1$.

The laser-driven DOS for quasi-2D electrons occupying the nth subband can now be determined from the imaginary part of the Fourier transform of this Green's function, i.e., $D_n(E)=-(g_s/\pi)\Sigma_{\mathbf{k}}\mathrm{Im}\{G^{*}_{n,\mathbf{k}}(E)\}$. Since $\mathbf{k}$ is a quasicontinuum vector, the usual conversion of the summation into a volume integral in the $\mathbf{k}$ space applies, leading to the following expression for the laser-driven DOS in the nth subband:

$$D_n(E) = \frac{2}{\pi}\rho_0 \sum_{m=0}^{\infty} \Theta(\overline{E}_{n\gamma m}) \int_0^1 \frac{d\xi}{\sqrt{1-\xi^2}} F_m^2\left(\xi\frac{\sqrt{2m^{*}\overline{E}_{n\gamma m}}}{\hbar}\right), \tag{19}$$

where $\overline{E}_{n\gamma m} \equiv E-\varepsilon_n-2\gamma\hbar\omega_x-m\hbar\omega_x$.

As pointed out elsewhere,[16,17] the processes of photon absorption and emission can induce strong changes in the DOS of quasi-2D electronic systems, mainly for laser field radiations with high intensity (i.e., large F_{0x}) and low frequencies (ω_x). There is, however, a lack of systematic investigation on the occurrence of such changes in the specific case of nonresonant laser fields,[19] and we think it may be due to the apparent contradiction in inducing changes in the 2D DOS (thus in the optical properties of the heterostructure) with nonresonant photons. Nevertheless, this is not true for a carrier system whose dimensionality can be reduced by applying an ILF on the QW structure, as we are reporting in this paper. In the case of a nonresonant laser beam, if the radiation frequency is such that $\omega_x\tau \gg 1$, then the rapid oscillation of the Bessel functions will make their integral null and only the term corresponding to $m=0$ in Eq. (19) will survive, thus reducing the summation to only one term. Explicitly, the DOS per unit area in the nth subband results

$$D_n(E) = \frac{2}{\pi}\rho_0\Theta(E-\varepsilon_n-2\gamma\hbar\omega_x) \times \int_0^1 \frac{d\xi}{\sqrt{1-\xi^2}} F_0^2\left(\xi\frac{\sqrt{2m^{*}(E-\varepsilon_n-2\gamma\hbar\omega_x)}}{\hbar}\right), \tag{20}$$

where $F_0(k_x)=J_0(\gamma)J_0(\alpha_{0x}k_x)+2\Sigma_{l>0,\mathrm{even}}J_l(\gamma)J_{2l}(\alpha_{0x}k_x)$ depends on both the laser intensity and frequency. Note that the total DOS, i.e., $D(E)$, is easily obtained from $D_n(E)$ as stated above, by doing

$$D(E) = \sum_n D_n(E). \tag{21}$$

In the low-field and /or high-frequency limits, both laser parameters γ and α_{0x} tend to zero and thus $F_0(k_x)\to 1$ since $\lim_{x\to 0}J_n(x)=\delta_{n,0}$. In this case, the DOS recovers its usual ladder profile in the absence of external fields, as stated in Eq. (4).

III. RESULTS AND DISCUSSIONS

As pointed out in Ref. 6, the interaction of a 2DEG with an intense laser field (ILF) results in blueshifts for all bound state energy levels due to the DFKE for both resonant and nonresonant radiation fields with in-plane polarization. Nevertheless, the possibility of inducing such shifts with nonresonant, intense laser fields polarized perpendicularly to the confinement layer (i.e., the QW channel) was not established. We analyzed this possibility here by developing extensive numerical calculations for electrons in a $GaAs/Al_xGa_{1-x}As$ single QW subjected to a monochromatic CO_2 laser beam polarized along the z axis and propagating in the y-axis direction with frequency $\omega_z=1.78\times10^{14}$ Hz and amplitude $F_{0z}=180$ kV/cm. With these laser parameters, the laser-dressing parameter (α_{0z}) evaluates to $\sim$15 Å. We took, for a $GaAs/Al_xGa_{1-x}As$ QW, a band gap of 1.519 eV between the conduction and valence bands in the GaAs layer, a band offset $V_0(x)=60\%\ \Delta E_{gap}$, where $\Delta E_{gap}=1.155x+0.37x^2$(eV), and assumed $m_A^{*}=0.0665m_0$ and $m_B^{*}=m_A^{*}+(0.1006x+0.0137x^2)m_0$ for the electron effective masses in the GaAs channel and in the $Al_xGa_{1-x}As$ barriers, respectively. By assuming[29] an electron mobility of $\sim 5\times10^6$ cm^2/V s we found $\omega_z\tau\sim 9535$ for $x=0.3$ ($V_0=227.9$ meV) which assures the validity of the approximations assumed in the laser-dressed potential approach [see Eqs. (6) and (7)]. For this Al molar fraction the nonresonance condition[19] is guaranteed only for well widths below

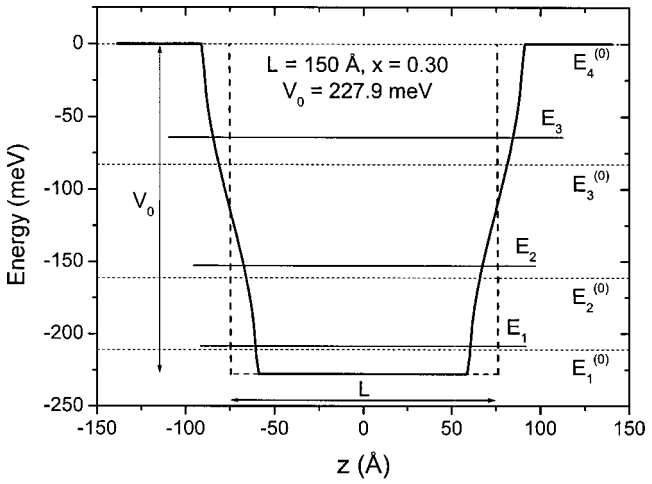

FIG. 2. Modifications in the conduction band edge and bound state energy levels for a 150-Å-wide $GaAs/Al_{0.3}Ga_{0.7}As$ single QW induced by an intense CO_2 laser field polarized parallel to the growth axis (z axis). The dashed lines represent the energies in the absence of external fields. The solid lines are for $F_{0z}=180$ kV/cm, corresponding to a laser-dressing parameter $\alpha_{0z}\sim 15$ Å. Note the fourth bound state energy level, initially just below the barriers, is made unbound as a consequence of the changes in the effective potential.

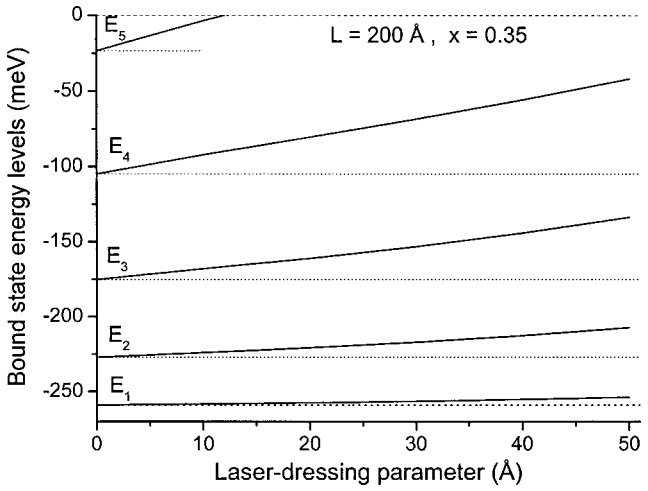

FIG. 3. Blueshifts induced by an intense CO_2 laser field on the bound state energy levels for a 200-Å-wide $GaAs/Al_{0.35}Ga_{0.65}As$ single QW as a function of the laser-dressing parameter, which was modified only through the laser intensity. The behavior is almost linear, and the fifth energy level is made unbound for α_{0z} above ~ 11.5 Å.

$L_{max}=190$ Å. To this extent we chose a well width of 150 Å and calculated every bound state energy level exactly (in the absence of external fields), namely $E_1=15.911$ meV, $E_2=63.442$ meV, $E_3=140.721$ meV, and $E_4=227.787$ meV (these are the values with respect to the bottom of the well). These energy levels are plotted in Fig. 2, together with the conduction band edge. In the presence of the CO_2 laser field, the potential is changed near to the heterointerfaces positions, i.e., $z=-L/2$ and $z=+L/2$, and all energy eigenvalues are affected, being blueshifted. The first three energy levels are shifted by ~ 1.7 meV, 7.3 meV, and 18.2 meV. The fourth energy level, initially just below the conduction band edge in the barriers, becomes unbounded in consequence of the changes in the effective potential. The increase of the blueshifts in each bound state energy level with respect to the laser intensity was also investigated. By changing the QW parameters to $x=0.35$ and $L=200$ Å (for this particular Al molar fraction L_{max} increases to ~ 215 Å) in viewing to increase the number of bound states, we found a situation in which there were five bound states well below the conduction band edge in the barriers (see the dashed lines in Fig. 3). By increasing the CO_2 laser intensity, all the energy levels are affected presenting an almost linear increase with the laser-dressing parameter as shown in Fig. 3. Note that the shifts are greater for higher level indexes. Note also the fifth level is made unbound for a laser-dressing parameter of ~ 11.5 Å.

So far, to our knowledge, the consequences of subjecting the carriers to an additional ILF in a crossed configuration, as shown in Fig. 1, was not yet investigated. We considered here the additional ILF as being a nonresonant THz laser ($\omega_x/2\pi=1\times 10^{12}$ Hz) polarized along the x axis and propagating along the z axis. According to previous works,[16,17] the effect of such ILF on the 2D DOS is remarkable in the case of resonant photons where the process of photon absorption is the main channel for electron-photon interactions. This feature results in a functional form for the electron DOS in terms of the laser intensity and frequency, but the occurrence of such form is not clear for *nonresonant* ILF. The inclusion of the effects of the nonresonant THz laser field in our model led to an additional feature, namely the blueshifts (DFKE) in the bound state energy levels, and there is also an important difference as compared with the ones calculated with the CO_2 laser acting alone[16,17] in which all energy levels are shifted by the same amount that corresponds to the energy of the EM radiation field, given by $2\gamma\hbar\omega_x$. For $F_{0x}=5$ kV/cm (15 kV/cm), we found additional blueshifts of 4.15 meV (37.02 meV) in all energy levels due to the presence of the THz ILF.

Bringing our attention back to the 150-Å-wide $GaAs/Al_{0.3}Ga_{0.7}As$ QW (Fig. 2), we investigated the changes induced on both the bound state energy levels and the electron DOS by these two crossed ILF radiation beams. The changes in the DOS with respect to the usual ladder profile are depicted in Fig. 4. It is clear from this graph that the effect of the THz laser field is to reduce it with respect to the free fields DOS (dashed line). The laser-driven DOS (solid lines) is seen to depend on the energy level and on the laser intensity according to a functional form. The reduction observed in the DOS for $F_{0x}=5$ kV/cm is only reasonable, but it becomes significant for $F_{0x}=15$ kV/cm. In fact, we verified that the DOS reduction due to the THz ILF enhances with the laser intensity monotonically, and it suggests an interesting tuning mechanism for the DOS dependency on the energy. There is also an interesting dependency for DOS on the laser frequency. This is depicted in Fig. 5, where the curves for a fixed CO_2 laser and an additional, crossed, THz laser field (with three different frequencies) are plotted. Note the blueshifts induced by the THz laser fields on the ground

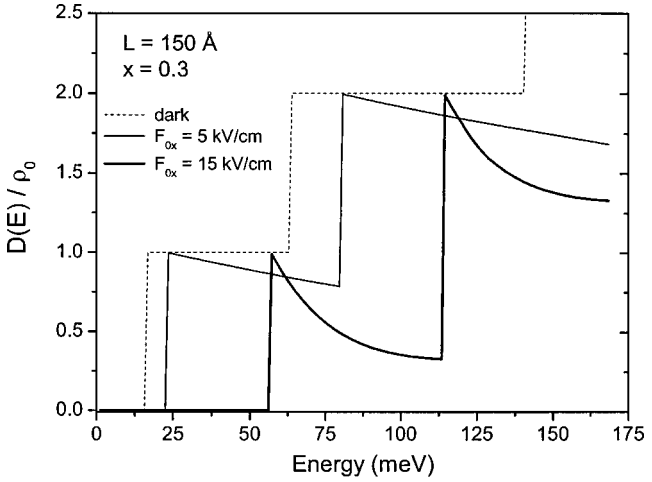

FIG. 4. The DOS for electrons confined in a 150-Å-wide $GaAs/Al_{0.3}Ga_{0.7}As$ single QW illuminated by two crossed ILFs. The EM radiation propagating along the y axis is an intense CO_2 laser field polarized parallel to the growth direction (i.e.,$F_z\hat{z}$), whereas the one propagating along the z axis is an intense THz laser field ($\omega_x/2\pi=1.0$ THz) polarized along the x axis (i.e., $F_x\hat{x}$). The dashed line is for the DOS in the absence of external fields. The other (solid) lines are for $F_{0z}=180$ kV/cm. The thinner (thicker) line is for $F_{0x}=5(15)$ kV/cm, with an additional (DFKE) blueshift of 4.15(37.02) meV due to the THz laser field.

state energy level increase with the reduction of the frequency, as expected for the DFKE-induced blueshift [i.e., $e^2F_{0x}^2/4m^*\omega_x$]. Moreover, the peak for the thicker solid line is clearly below 1.0, a fact that is easy to be understood whether the factor $J_0^2(\gamma)$, implicit in the expression of $D_n(E)$ in Eq. (20), with $F_0(k_x)\cong J_0(\gamma)J_0(\alpha_{0x}k_x)$, is taken into account. First, at the DOS discontinuities we have $E=\varepsilon_n+2\gamma\hbar\omega_x$, thus the argument of the function F_0^2 is null. This reduces the integral to just $\int_0^1 d\xi/\sqrt{1-\xi^2}$, which has an exact value, namely $\pi/2$, and this makes the DOS at the discontinuity (in units of ρ_0) to be proportional to $J_0^2(\gamma)$. Since, for a given F_{0x}, γ increases with $1/\omega_x^3$ for decreasing values of ω_x, $J_0^2(\gamma)$ is just below 1.0 for small values of γ, but diminishes rapidly for $\gamma>0.5$ [e.g., $J_0^2(0.5)\cong 0.88$ but $J_0^2(0.9)\cong 0.65$]. This is the reason for the DOS peak to stay far below 1.0 for the smaller ω_x. The DOS dependencies on the laser intensity and frequency we investigated here are important since the DOS reflects the maximum number of carriers that can occupy states with energies between E and $E+dE$, thereby affecting the Fermi level calculation intrinsically.[16,17] As the 2DEG density in modulation-doped QWs is strongly dependent on the Fermi level position with respect to the subband energy levels this laser-dressed DOS tuning should alter the charge transfer process, as pointed out in previous works.[13,16,17] We noted that the THz-laser-driven electron DOS we obtained with nonresonant photons is somewhat different from the one obtained previously for the case of m-photon absorption[17] in which the photon emission was observed to be a secondary channel for electron-photon interactions. Firstly, the blueshift obtained for a THz laser field with intensity of 4 kV/cm is only ~2.5 meV for all energy levels whereas those we found are much higher and increase with the index of the energy level due to the presence of the second, extra CO_2 ILF. This can be seen in Fig. 4 by comparing the distances between each vertical solid line (discontinuity at $E=E_n$) and its respective vertical dashed line (discontinuity at $E=E_n^{(0)}$), which refers to the bound state energy levels in the absence of external fields. For $F_{0x}=5(15)$ kV/cm we obtained total blueshifts of 6.35 meV and 13.25 meV (39.22 and 41.17 meV), respectively. Secondly, provided the lasers we used here were taken nonresonant with the carriers energy states, the oscillations obtained in the DOS dependence on energy with a resonant THz laser[17] have not been observed although the increase in the DOS reduction for increasing laser intensities is almost the same.[6,17] The lack of such oscillations may be explained in terms of the nature of the electron-photon interaction for nonresonant photons as follows. In the presence of resonant photons, the opening of additional channels for optical absorption ($m>0$) and emission ($m<0$) leads to a non-null $D_n(E)$ for $E-E_n<0$ and to an increase in the DOS which can make $D_n(E)$ larger than ρ_0 (see, e.g., Ref. 16). These features are not present in our results since in the case of a nonresonant ILF the series (involving Bessel functions of several orders) established for the averaged Green's function $G_{n,\mathbf{k}}^*(E)$ in Eq. (18), which is the "heart" of the DOS in the nth subband given by Eq. (19), is reduced to only one term (i.e., the term corresponding to $m=0$) due to the absence of resonant photons ($m\neq 0$). In this way, there remains only $F_0(k_x)$, which is a series involving Bessel functions of even order. We verified that for THz laser intensities below 20 kV/cm, the zeroth order term dominates entirely the behavior in such a way that $F_0(k_x)\cong J_0(\gamma)J_0(\alpha_{0x}k_x)$ represents a very reasonable approximation. We checked it out by computing the DOS with the entire series truncated at the term of order 16

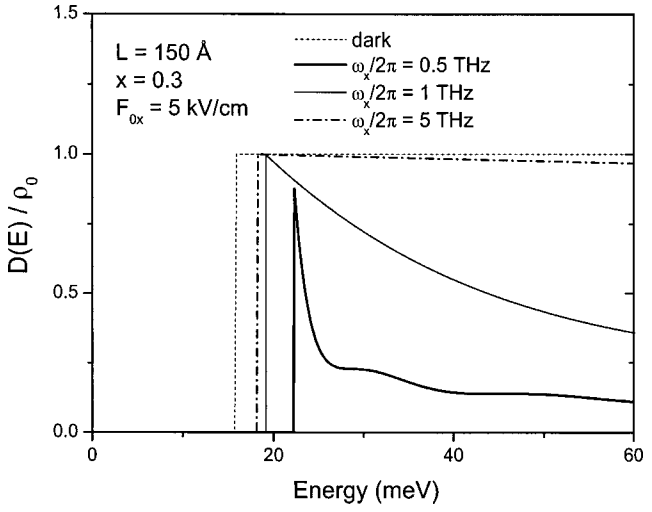

FIG. 5. The DOS for electrons confined in a 150-Å wide $GaAs/Al_{0.3}Ga_{0.7}As$ single QW illuminated by two crossed, ILFs. The dashed line is for the DOS in the absence of external fields. The other lines are for $F_{0z}=180$ kV/cm and $F_{0x}=5$ kV/cm (CO_2 and THz laser sources, respectively). The thicker (thinner) solid line is for $\omega_x/2\pi=0.5(1.0)$ THz. The dash-dotted line is for $\omega_x/2\pi=5$ THz. Emphasis is given for the DOS around the ground state energy.

for many THz laser intensities and then comparing these accurate results with the ones obtained with the above zeroth order approximation. We did not detect any significant differences whatsoever, which makes clear that the oscillations in the DOS are provoked by the terms with $m \neq 0$ in the series of $G^{*}_{n,\mathbf{k}}(E)$ associated with the resonant photons, not considered in our present simulations, and not by the exclusion of high-order terms in the summation for $F_0(k_x)$. It is interesting to note that the laser-reduced DOS is strongly dependent on the THz laser intensity, which suggests a simple optical tuning mechanism for such quantity. Moreover, the blueshifts are significantly enhanced as a consequence of both THz and CO_2 lasers making it possible to tune the bound state energy levels efficiently in a broad range by using the present laser-crossed configuration.

It is also important to emphasize that we analyzed the effects of intense lasers only on GaAs/AlGaAs quantum wells, but it should not be difficult to extend the results to other semiconductor materials with zinc-blend structure, such as other III-V and III-nitride compounds, as long as the parameters used here for GaAs/AlGaAs QWs be adjusted for these materials. In this case, different values of L_{max} will arise and they should be considered strictly in order to keep the approximations assumed here valid.

IV. CONCLUSIONS

In closing, we investigated systematically the changes induced by intense, long-wavelength, nonresonant laser fields on some electronic properties, namely the bound state energy levels and the electron DOS for quasi-2D electrons in a single undoped GaAs/AlGaAs quantum well. Our results show that the effect of such laser fields on the bound state energy levels is to induce blueshifts, which depend on the laser intensity and frequency as well as on the polarization direction. For a CO_2 ILF polarized along the growth direction, the dependence on the laser intensity is monotonic, the blueshifts being larger for higher lying energy levels. Our numerical results pointed out that the excited energy levels can be made unbound for some critical laser intensity. Their dependence on the laser frequency and polarization was investigated by comparing the effect of such CO_2 ILF with that of an in-plane polarized THz ILF. The blueshift induced by the THz ILF is the same for all energy levels being equal to the energy of the EM radiation field $(2\gamma\hbar\omega_x)$. We found linear dependencies of the blueshifts on the laser-dressing parameter for both ILF polarizations, which suggests an interesting optical mechanism for tuning all bound state energy levels.

For the electron DOS dependency on energy in the presence of a nonresonant in-plane polarized THz laser field, we found reductions that depend on the THz laser intensity and frequency. The smooth and monotonic increase of such reduction with the THz laser intensity suggests an interesting tuning mechanism for the electron DOS, Fermi level, and 2DEG density, as previously established for resonant ILFs.[13,16,17] In particular, the DOS changes from the usual steplike shape to a functional form, which reminds one of a quantum wire (1D DOS). It is expected that these deformations in the laser-dressed DOS come to induce an increase in the Fermi energy for a fixed number of carriers, thereby altering their optical and transport properties. The understanding of the effects of intense, long-wavelength, nonresonant laser fields on the quasi-2D electron DOS and energy levels suggests to us a way for tuning such quantities by varying the laser frequency and intensity. This kind of optical control may be of great interest for those working with optoelectronic devices based on quantum wells or similar low-dimensional systems under intense laser fields conditions,[27–31] a research field that has been fueled by the present development of high-power pulsed laser fields, such as THz laser fields, as well as the building up of new low-dimensional structures.[32–34]

ACKNOWLEDGMENTS

O.A.C.N., E.F.D.S., Jr., and V.N.F. wish to thank the CNPq (Brazilian agency) for Doctor Research Grants during the course of this work. Thanks are also due to the Brazilian Network for Nanoscience (NanoSemiMat) for financial support during the course of this work. This work was partially supported by FINATEC (Brazilian agency).

*Electronic address: oacn@fis.unb.br

[1] A. G. Markelz, N. G. Asmar, B. Brar, and E. G. Gwinn, Appl. Phys. Lett. **69**, 3975 (1996).
[2] T. A. Vaughan, R. J. Nicholas, C. J. G. M. Langerak, B. N. Murdin, C. R. Pidgeon, N. J. Manson, and P. J. Walker, Phys. Rev. B **53**, 16 481 (1996).
[3] B. N. Murdin, W. Heiss, C. J. G. M. Langerak, S. C. Lee, I. Galbraith, G. Strasser, E. Gonik, M. Helm, and C. R. Pidgeon, Phys. Rev. B **55**, 5171 (1997).
[4] N. G. Asmar, A. G. Markelz, E. G. Gwinn, J. Cerne, M. S. Sherwin, K. L. Chapman, P. E. Hopkins, and A. C. Gossard, Phys. Rev. B **51**, 18 041 (1995); N. G. Asmar, J. Cerne, A. G. Markelz, E. G. Gwinn, M. S. Sherwin, P. E. Hopkins, and A. C. Gossard, Appl. Phys. Lett. **68**, 829 (1996).
[5] W. Xu and C. Zhang, Appl. Phys. Lett. **68**, 3305 (1996); Phys. Rev. B **54**, 4907 (1996); **55**, 5259 (1997).
[6] A. P. Jauho and K. Johnsen, Phys. Rev. Lett. **76**, 4576 (1996).
[7] C. R. Pidgeon, Infrared Phys. Technol. **40**, 231 (1999); N. H. Tolk, R. G. Albridge, A. V. Barnes, B. M. Barnes, J. L. Davidson, V. D. Gordon, G. Margaritondo, J. T. McKinley, G. A. Mensing, and J. Sturmann, Appl. Surf. Sci. **106**, 205 (1996).
[8] E. Gerck and L. C. M. Miranda, Appl. Phys. Lett. **44**, 837 (1984).
[9] R. M. O. Galvão and L. C. M. Miranda, J. Phys. C **17**, L41 (1984); X. L. Lei, J. Phys.: Condens. Matter **10**, 3201 (1998); C. Zhang, Phys. Rev. B **66**, 081105(R) (2002).
[10] Fanyao Qu, A. L. A. Fonseca, and O. A. C. Nunes, Superlattices Microstruct. **23**, 1005 (1998).
[11] J. C. Cao and X. L. Lei, Phys. Rev. B **67**, 085309 (2003).

[12] C. Zhang, Appl. Phys. Lett. **78**, 4187 (2001); E. C. Valadares, Phys. Rev. B **41**, 1282 (1990).
[13] E. C. Valadares, A. B. Henriques, J. R. Leite, and A. S. Chaves, Physica E (Amsterdam) **8**, 201 (1990); W. Xu and C. Zhang, Physica E (Amsterdam) **2**, 252 (1998).
[14] W. Xu, Phys. Rev. B **57**, 15282 (1998).
[15] J. Kono, M. Y. Su, T. Inoshita, T. Noda, M. S. Sherwin, S. J. Allen, and H. Sakaki, Phys. Rev. Lett. **79**, 1758 (1997); H. Nakano, H. Kubo, N. Mori, C. Hamaguchi, and L. Eaves, Physica E (Amsterdam) **7**, 555 (2000); N. Mori, T. Takahashi, T. Kambayashi, H. Kubo, C. Hamaguchi, L. Eaves, C. T. Foxon, A. Patane, and M. Henini, Physica B **314**, 431 (2002).
[16] W. Xu, Semicond. Sci. Technol. **12**, 1559 (1997).
[17] W. Xu, Europhys. Lett. **40**, 411 (1997).
[18] These expressions can be computed only numerically for a given set of quantum well and laser parameters.
[19] The nonresonance condition between the laser frequency and the QW structure was observed in all calculations in this paper. Such condition simply requires the laser frequency to be below the critical value for which the photon energy could reach any relevant transition energy for the carriers in the quantum well.
[20] V. V. Mitin, V. A. Kochelap, and M. A. Stroscio, *Quantum Heterostructures* (Cambridge University Press, Cambridge, 1999).
[21] G. Bastard, *Wave Mechanics Applied to Semiconductor Heterostructures* (Les Editons de Physique, Paris, 1988).
[22] J. H. Davies, *The Physics of Low-Dimensional Semiconductors* (Cambridge, New York, 1998).
[23] F. M. S. Lima, Ph.D. thesis, University of Brasilia, 2003 (unpublished).
[24] M. Gravila and J. Z. Kaminski, Phys. Rev. Lett. **52**, 613 (1984).
[25] M. Fujita, T. Toyoda, J. C. Cao, and C. Zhang, Phys. Rev. B **67**, 075105 (2003); C. Zhang, *ibid.* **65**, 153107 (2002).
[26] Fanyao Qu, A. L. A. Fonseca, and O. A. C. Nunes, Phys. Rev. B **54**, 16405 (1996).
[27] T. L. Li and K. J. Kuhn, J. Comput. Phys. **110**, 292 (1994).
[28] R. D. Mattuk, *A Guide to Feynman Diagrams in the Many-Body Problem* (McGraw-Hill, New York, 1976).
[29] F. M. S. Lima, Fanyao Qu, O. A. C. Nunes, and A. L. A. Fonseca, Phys. Status Solidi B **225**, 43 (2001); F. M. S. Lima, A. L. A. Fonseca, O. A. C. Nunes, and Fanyao Qu, J. Appl. Phys. **92**, 5296 (2002).
[30] S. Hughes and D. S. Citrin, J. Opt. Soc. Am. B **17**, 128 (2000).
[31] L. E. Oliveira, A. Latge, and H. S. Brandi, Phys. Status Solidi A **190**, 667 (2002).
[32] E. Schomburg, K. Hofbeck, R. Scheuerer, M. Haeussler, K. F. Renk, A. K. Jappsen, A. Amann, A. Wacker, E. Scholl, D. G. Pavel'ev, and Y. Koschurinov, Phys. Rev. B **65**, 155320 (2002); A. K. Jappsen, A. Amann, A. Wacker, E. Scholl, and E. Schomburg, J. Appl. Phys. **92**, 3137 (2002).
[33] H. Sari, E. Kasapoglu, and I. Sokomen, Phys. Lett. A **311**, 60 (2003).
[34] J. L. Nie, W. Xu, and L. B. Lin, Int. J. Mod. Phys. B **17**, 2487 (2003).